Realization of RF and Microwave Energy Harvesting System Adapted to GSM 900 Network for Low Power Consumption Sensors Feeding

Chemseddine Benkalfate
Electrical and Electronics Engineering Department, ENSEA
Quartz laboratory
Cergy, France
e-mail: benkalfate.chemseddine@ensea.fr

Achour Ouslimani
Electrical and Electronics Engineering Department, ENSEA
Quartz laboratory
Cergy, France
e-mail: achour.ouslimani@ensea.fr

Abed-Elhak Kasbari
Electrical and Electronics Engineering Department, ENSEA
Quartz laboratory
Cergy, France
e-mail: abed-elhak.kasbari@ensea.fr

Mohammed Feham
Telecommunication Department, University of Tlemcen
STIC laboratory
Tlemcen, Algeria
e-mail: feham_m@yahoo.fr

***Abstract*— This paper presents a miniaturized Radio-Frequency (RF) and microwave energy harvesting system adapted to GSM-900 Network (Global System for Mobile Communication). Most researchers have worked in this domain by trying to harvest an enough DC output voltage to feed different electronic devices to ensure their energy autonomy. The matter with these systems lies in the antenna size. The proposed system is realized on Teflon hybrid technology. The size of the proposed multiband antenna is of 20x30x0.67 mm^3, and that of the rectifier matched to the antenna is of 10x15x0.67 mm^3. The measurement shows that the antenna is able to cover GSM900 (935 – 960) MHz, (1470 – 1550) MHz, GSM1900 (1935 – 1989) MHz and (3 – 3.2) GHz, bands. The output Direct Current (DC) harvested voltage measured is of 0.3 V for 2 kΩ resistance load. This result is sufficient for feeding low power consumption Wireless Sensor Networks (WSNs). In this paper, the selected temperature sensor operates for 0.2 V and 23 nW power supply. The equivalent resistor of this sensor is 2 kΩ. The DC output voltage can reach 0.8 V for open load.**

Keywords--RF Energy harvesting; Multi-bandes antenna; Miniaturized antenna; Impedance matching; Rectifier.

I. INTRODUCTION

The RF and micro-wave energy harvesting devices consist of 3 primary blocks, antenna, impedance matching and rectifier (see Figure 1). The antenna is a primordial device on these systems, which is a responsible of all electromagnetic waves catching from the environment with adapting frequencies and power levels. Antennas which allow to capture many waves at many frequency bandwidths improve widely the RF and microwave energy harvesting system performances. The proposed antenna is smallest (20x30x0.67 mm^3) compared to the GSM antennas (GSM-900, GSM-1800/1900) commonly used with keeping a high efficiency levels [7]. This answers to recommended miniaturization required for the harvesting systems [4][5]. The rectifier is matched to the antenna by using an impedance matching network, which is realized with Surface Mounted Devices (SMD) electronic elements (inductors and capacitors). The rectifier is based on Schottky diode (MBRS360T3G) and capacitor voltage doubler [5][8]. The dimension of the proposed RF and microwave energy harvesting circuit is of 10x15x0.67 mm^3. This miniaturized system could be used to power many applications (sensors, smart watches, etc.).

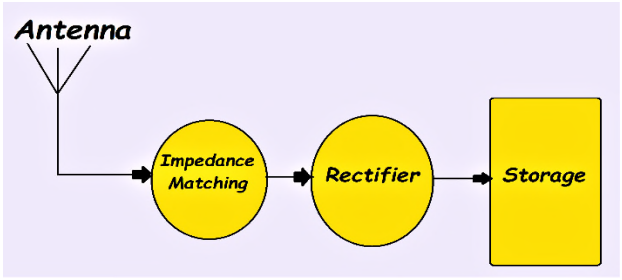

Figure 1. General RF energy harvesting system blocks [1].

II. ANTENNA SIMULATION CHARACTERISTICS

A. Antenna structure

Figure 2, depicts the proposed antenna structure.

 ISBN: 978-1-61208-828-0

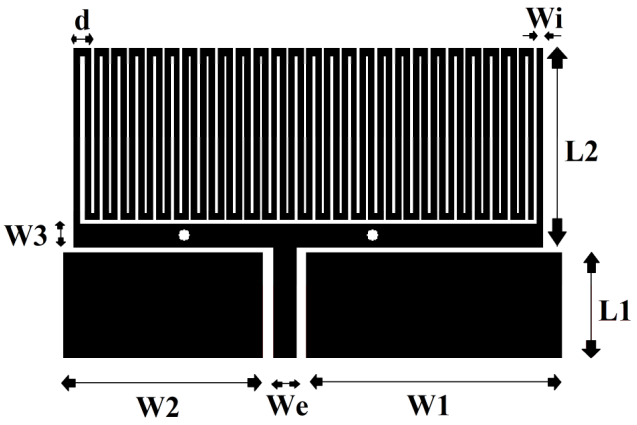

Figure 2. The proposed antenna structure .

The reported antenna in [10] is modified to cover multiband frequency by adding many meanders, which mean many bands. Each meander can be modeled electrically by inductors [3]. Table I presents the antenna dimensions in mm.

TABLE I. ANTENNA DIMENSIONS

L_1	L_2	W1	W2	W3	We	Wi	d
6	14	17	9	4	2	1.5	2

B. Antenna Response And Radiation Diagram

Figures 3 and 4 present respectively the return loss of this antenna and the radiation diagram getting by exploring the Computer Simulation Technology (CST) software.

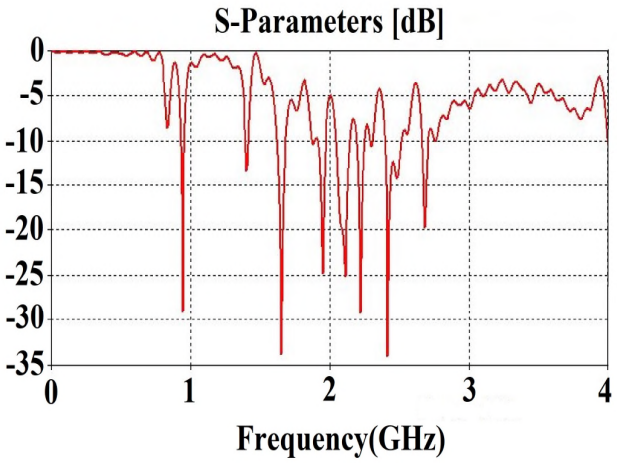

Figure 3. Simulated S_{11} antenna response.

we clearly see that this antenna is operational within the frequency bandwidths, (945 – 960) MHz with S11≤ -25 dB, (1780 – 1850) MHz with S11≤ -30dB, (1930 – 1980) MHz with S11≤ -25dB, (2450 – 2500) MHz with S11≤ -25dB and (2610 – 2680) MHz with S11≤ -20dB,

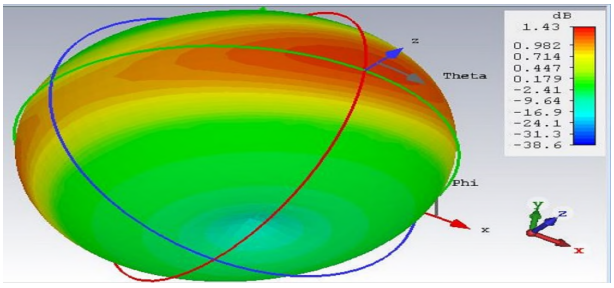

Figure 4. Radiation diagram at 948 MHz, 1.8 GHz, 1.96 GHz.

the radiation diagram of this antenna is omnidirectional, that is flawlessly tailored to the mobile communication GSM900, GSM1800 and GSM1900 (PCS network), the gain is around 1.43dB, 1.38 in linear scale.

C. Antenna Stability

The stability of this antenna is handled very cautiously by adjusting with precision its dimensions [9]-[11]. Figure 5 shows the smith-chart, in which the stability of this antenna appears when the graph stays inside the principal smith chart circle, as we can see, this antenna is within the stability restriction, because the S11 curve contacts the unit circle but it doesn't exceed it, in invers case we talk about the antenna instability. This analysis is imperative for such an antenna. Otherwise, the measured response might be definitely different from the simulations. The performance could then decrease drastically.

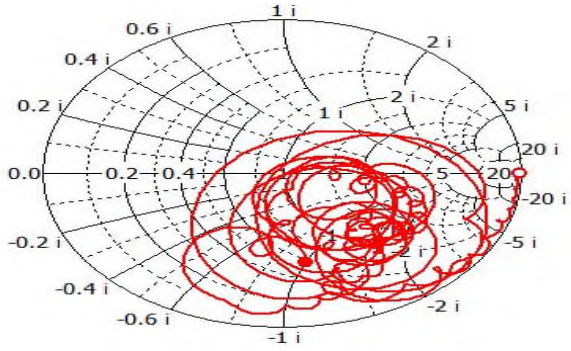

Figure 5. Smith chart representation.

D. Cosimulation Results

By using Advanced Design Systems (ADS) software (see Figure 6), the co-simulation response is depicted in the Figure 7.

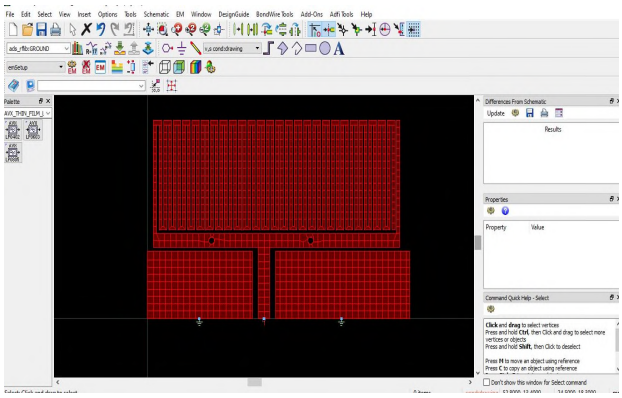

Figure 6. presented antenna model on ADS.

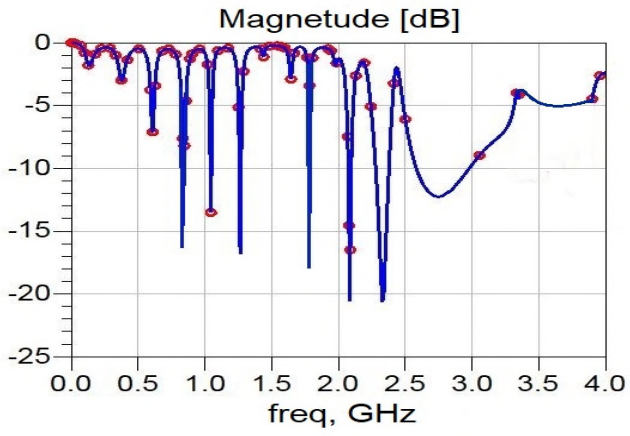

Figure 7. Proposed antenna co-simulation response.

In Figure 7, it is clear that the co-simulation response is in good agreement with that of the electromagnetic simulation obtained using CST software (see Figure 3).

E. Antenna Electrical Equivalent Circuit

As we noted in Section II-A, this antenna is formed from many LC resonators, theoretically [3], the meandered antennas models can be translated electrically to a superposition of many LC resonators as presented in the Figure 8. These resonator successions allow to have a multi-bands antenna, in level of sum resonators. The electromagnetic coupling phenomena are possible, due to the same resonance frequency of sum resonators.

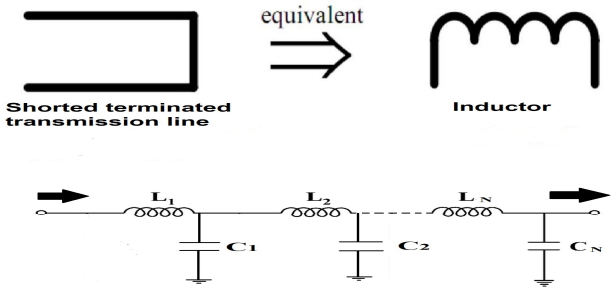

Figure 8. Equivalent electrical element.

We simulate the response of this antenna equivalent circuit on ADS. The proposed model is depicted in Figure 9, and its response in Figure 10.

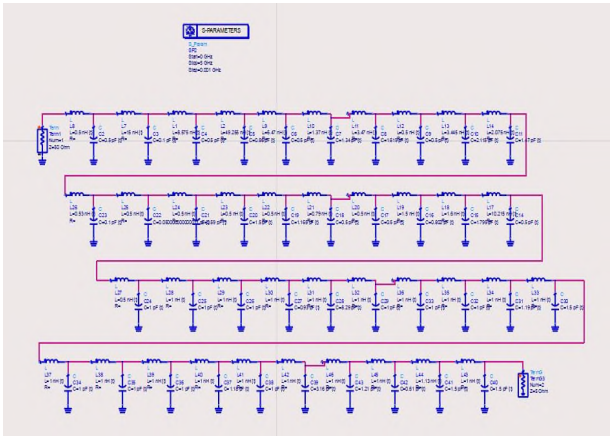

Figure 9. Equivalent electrical circuit on ADS software.

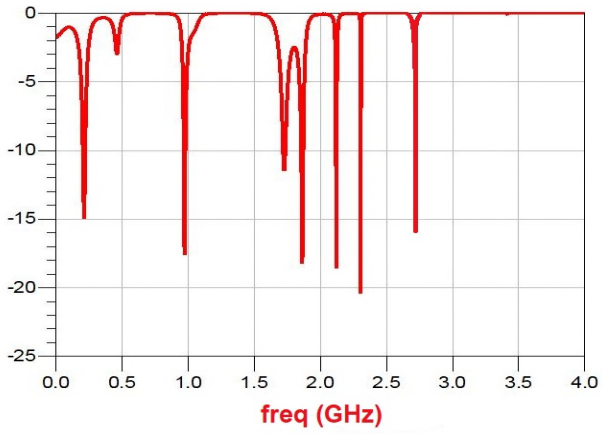

Figure 10. Antenna electrical equivalent circuit response.

 ISBN: 978-1-61208-828-0

We can clearly see in Figure 10, the electrical equivalent circuit response is too adapted to the simulation and co-simulation one, such as, for GSM900 band (950-960) MHz the S11 ⩽ -15 dB, GSM1900 (PSC) the S11 ⩽ -15 dB, UMTS2100 S11⩽-15 dB, Wi-Fi 2.45 GHz S11⩽-20 dB, LTE 2.6 GHz S11⩽-15 dB.

III. REALIZED ANTENNA AND MEASUREMENT

A. Realized Antenna Model

The proposed antenna structure represented in Figure 11, is printed on Teflon substrate (εr=2.1) with a dimension of 20 x 30 x 0.67 mm^3.

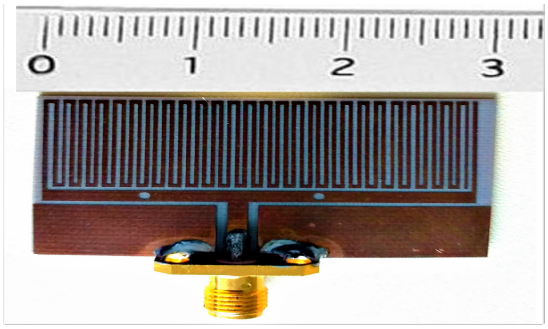

Figure 11. Realized antenna model.

B. Measured Response

Figure 12 shows the S_{11} parameter measured on vector network analyzer.

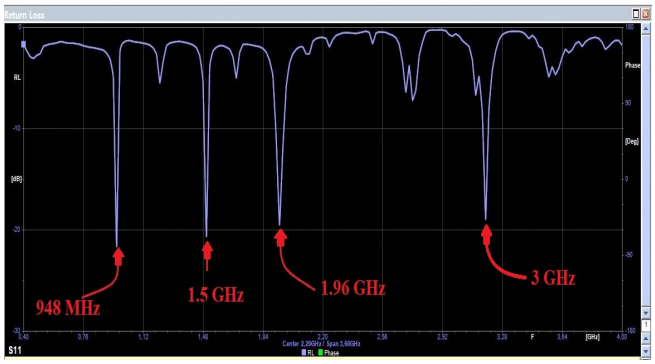

Figure 12. Measured antenna response.

In Figure 12, we see that this antenna is perfectly matched to GSM-900 and GSM-1900 bands. At the frequency 948 MHz the S_{11} is less than -20 dB and equal to -19 dB for 1.96 GHz frequency, there are two other resonance frequencies, at 1.5 GHz and 3 GHz with an S_{11} less than -18 dB.

IV. RECTIFIER AND IMPEDANCE MATCHING CIRCUITS

C. Proposed Rectifier

The rectification circuit has the function of transforming an alternating signal into another continuous. The proposed circuit is designed based on Schottky diodes (MBRS360T3G), and two capacitors connected in parallel which allows to double the output DC voltage. Figure 13 shows the proposed rectification circuit.

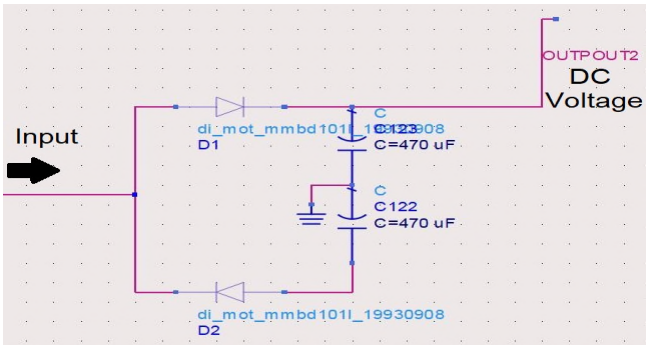

Figure 13. The proposed rectifier.

An impedance matching circuit is required to match this circuit to the antenna. The first step is to calculate the equivalent impedance of the rectifier, by using ADS software and streaming Smith chart. Figure 14 depicts the value of this impedance. At this level, we know both impedance va-

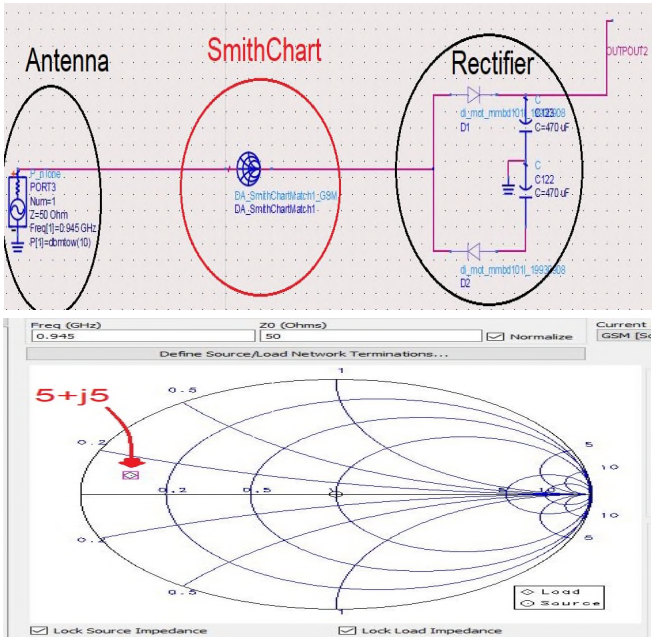

Figure 14. Smith Chart Presentation (Zeq = 5+j5).

lues, 50 Ohm for the antenna and 5+j5 Ohm for the rectifier. Now, we can design the impedance matching circuit between both sides (antenna and rectifier).

D. Proposed Impedance Matching

Figure 15 shows the proposed model designed on ADS software.

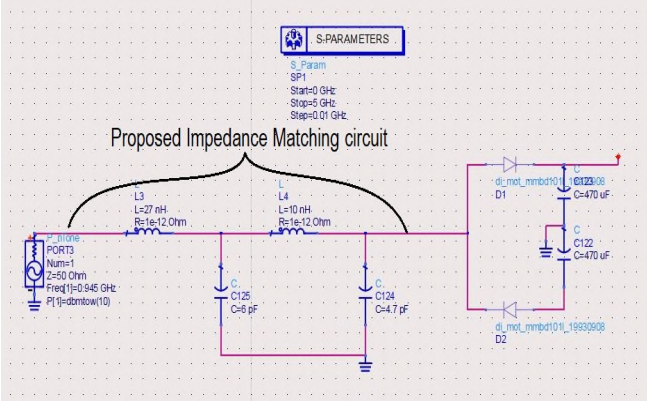

Figure 15. Proposed impedance matching circuit.

For adapting this circuit to GSM-900, we use Smith chart on ADS software, which is presented in Figure 16.

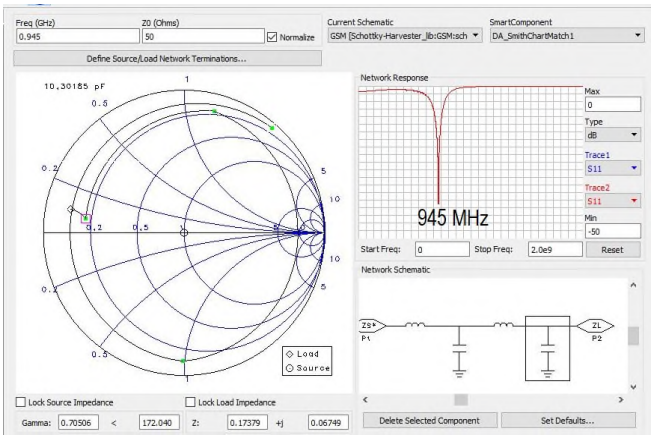

Figure 16. Impedance matching circuit S11.

We can clearly see that the proposed circuit is too adapted to GSM-900 at 945 MHz, the value of each elements is tuned by ADS, we can also calculate them by using the resonance formula.

E. Simulated Output DC Voltage

Figure 17 presents simulated output voltage for -40 dBm input power.

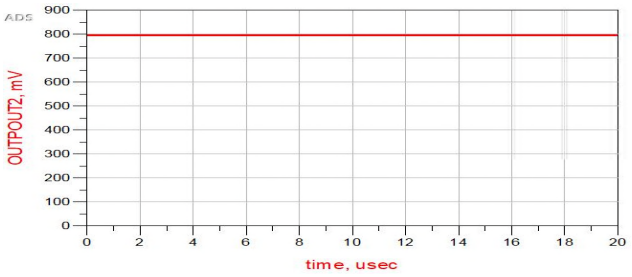

Figure 17. DC output voltage for -40 dBm input power

From this result, the harvested DC voltage is 0.8 V, simulated on ADS without termination load. This system is designed to feed low power consumption Wireless Sensor Networks (WSNs). The temperature sensor of [2] is operational for 0.2V and its equivalent resistance is 2 kΩ. Figures 18 and 19 show the proposed system with sensor load termination and its simulated DC output voltage, respectively.

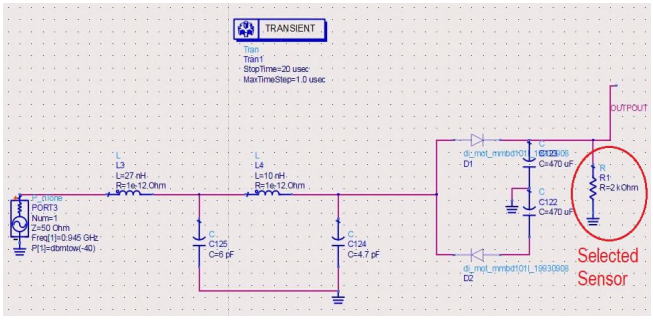

Figure 18. The proposed RF energy harvesting system with 2 kΩ load.

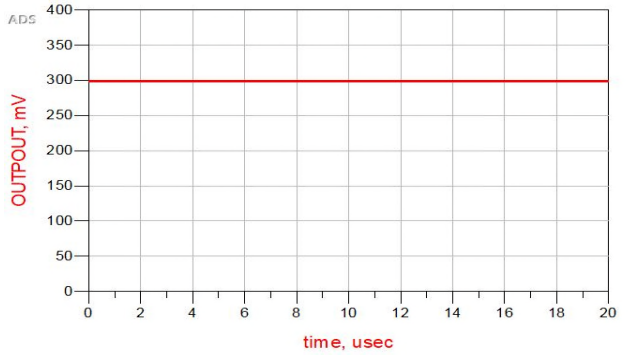

Figure 19. DC output voltage for -40 dBm input power and 2kΩ load.

 ISBN: 978-1-61208-828-0

The output DC voltage is 0.3V, which is enough for feeding the selected temperature sensor of [2].

V. SYSTEM REALISATION AND MEASUREMENT

A. Model Realization

Figure 20 presents the realized RF energy harvesting circuit (impedance matching + rectifier circuits).

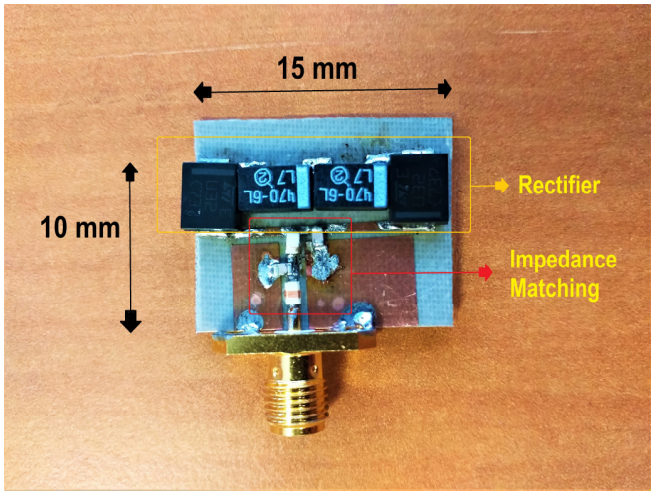

Figure 20. Proposed RF energy harvesting circuit (Impedance matching + Rectifier circuits).

B. S_{11} circuit Measurement

Figure 21 depicts the measured return loss.

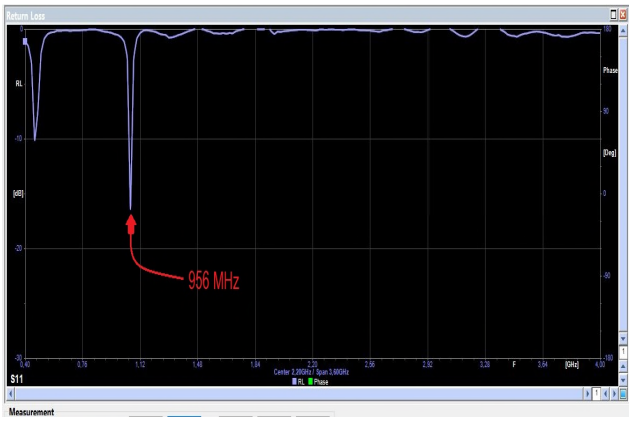

Figure 21. RF energy harvesting circuit return loss measurement.

As shown in Figure 21, the return loss is centered at 958 MHz, therefore, this circuit is adapted to GSM-900 downlink band.

C. Measured DC output voltage

Figure 22 shows the realized system (Antenna + RF energy circuit).

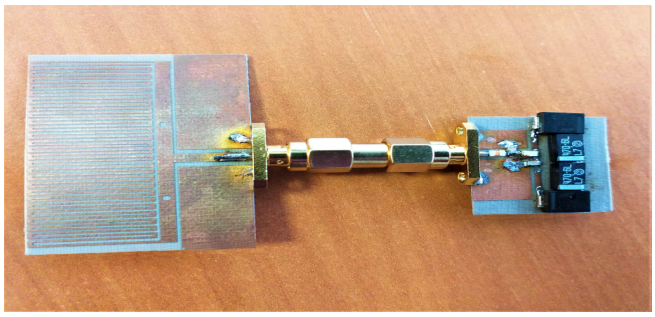

Figure 22. Realized proposed system.

The DC output voltage measurement has been achieved by using a Multimeter and an Oscilloscope. Figures 23 and 24 show the obtained results.

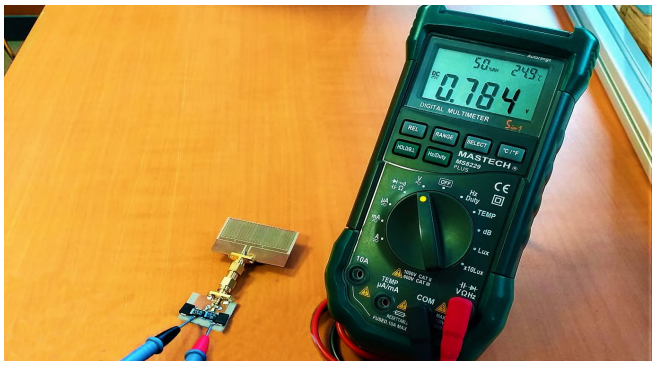

Figure 23. Measured output DC voltage using multimeter.

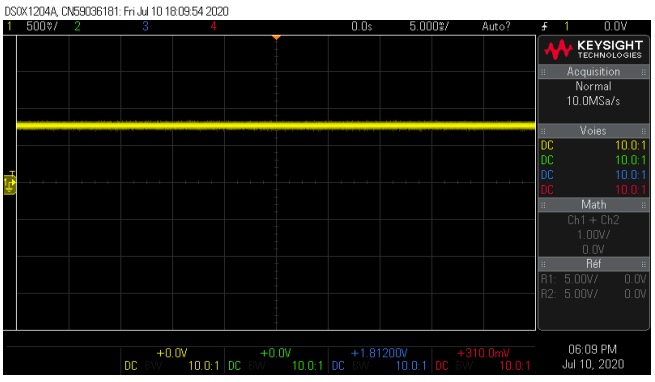

Figure 24. Measured output DC voltage using Oscilloscope with 500 mV per Division.

We can see that the measured output DC voltage is too near from that of the simulation one with 0.8 V, which

confirms that the simulation and measurement are in good agreement. This proposed system can perfectly feed the low power consumption temperature sensor in [2], which requires 0.2 V for working.

VI. CONCLUSION

In this work, we proved that is possible to feed low power consumption electronic devices (sensors, Radio-cognitive devices, smart watches, etc.) using RF and microwave energy harvesting systems, by exploring all mobile communication and wireless networks. A circuit adapted to GSM 900 network is proposed for feeding a low power consumption temperature sensor reported in [2], and by exploring more mobile communication networks more we increase the DC output voltage. The realized antenna and RF and microwave energy harvesting circuit (impedance matching + rectifier) are miniature with a dimension of 20x30x0.67 mm^3 and 10x15x0.67 mm^3, respectively. The harvested DC voltage from GSM-900 is 0.8 V for open load termination and 0.3 V for 2 kΩ resistance load, which is the sensor equivalent resistance.

REFERENCES

[1] C. Benkalfate, M. Feham, A. Ouslimani and A. Kasbari, "Investigation on the RF and Microwave Energy Harvesting from wireless and mobile communication networks," 2019 International Symposium on Networks, Computers and Communications (ISNCC), Istanbul, Turkey, 2019, pp. 1-6, doi: 10.1109/ISNCC.2019.8909092.

[2] A. Kamakshi; A. Shrivastava and B.H Calhoun. "A 0.2 V, 23 nW CMOS Temperature Sensor for Ultra-Low-Power IoT Applications". *J. Low Power Electron. Appl.* 2016, pp. 1-16, doi: 10.3390/jlpea6020010.

[3] A. Das, S. Dhar and B. Gupta, "Lumped circuit model analysis of meander line antennas," 2011 11th Mediterranean Microwave Symposium (MMS), Hammamet, 2011, pp. 21-24, doi: 10.1109/MMS.2011.6068520.

[4] N. Pournoori, M. W. A. Khan, L. Ukkonen and T. Björninen, "RF Energy Harvesting System Integrating a Passive UHF RFID Tag as a Charge Storage Indicator," 2018 IEEE International Symposium on Antennas and Propagation & USNC/URSI National Radio Science Meeting, Boston, MA, 2018, pp. 685-686, doi: 10.1109/APUSNCURSINRSM.2018.8608530.

[5] P. Sivagami, M. Pushpavalli, P. Abirami, S. Sindhuja and N. S. Reddy, "Implementation Of RF Energy Harvesting For Mobile Charging," 2018 IEEE International Conference on Computational Intelligence and Computing Research (ICCIC), Madurai, India, 2018, pp. 1-4, doi: 10.1109/ICCIC.2018.8782427.

[6] R. K. Sidhu, J. Singh Ubhi and A. Aggarwal, "A Survey Study of Different RF Energy Sources for RF Energy Harvesting," 2019 International Conference on Automation, Computational and Technology Management (ICACTM), London, United Kingdom, 2019, pp. 530-533, doi: 10.1109/ICACTM.2019.8776726.

[7] L. Lizzi, F. Ferrero, J. Ribero and R. Staraj, "Light and Low-Profile GSM Omnidirectional Antenna," in IEEE Antennas and Wireless Propagation Letters, vol. 11, pp. 1146-1149, 2012, doi: 10.1109/LAWP.2012.2219291.

[8] R. Suryadevara, T. Li, K. Modepalli and L. Parsa, "High-gain soft-switching DC-DC converter with voltage-doubler rectifier modules," 2017 IEEE Energy Conversion Congress and Exposition (ECCE), Cincinnati, OH, 2017, pp. 5692-5697, doi: 10.1109/ECCE.2017.8096946.

[9] V. Bande, P. T. R. Kumar and K. Krishnamoorthy, "Dual Band-Dual Sense Circularly Polarized Patch Antenna for Wi-Max Application," 2018 IEEE Indian Conference on Antennas and Propogation (InCAP), Hyderabad, India, 2018, pp. 1-4, doi: 10.1109/INCAP.2018.8770719.

[10] C. Huang, Y. Jiao, Z. Weng and X. Li, "A planar multiband antenna based on CRLH-TL ZOR for 4G compact mobile terminal applications," 2018 International Workshop on Antenna Technology (iWAT), Nanjing, 2018, pp. 1-3, doi: 10.1109/IWAT.2018.8379200.

[11] L. Shen, H. Wang, N. Hojjat, W. Lotz and H. Jamali, "Dual-Polarized Wideband Remote Electrical Tilt Multi-Beam Antennas," 2018 IEEE International Symposium on Antennas and Propagation & USNC/URSI National Radio Science Meeting, Boston, MA, 2018, pp. 2225-2226, doi: 10.1109/APUSNCURSINRSM.2018.8608298.

[12] C. Tienda, A. Katsounaros and S. Stirland, "Dual Reflectarray Ka-band Multibeam Antenna," 2019 13th European Conference on Antennas and Propagation (EuCAP), Krakow, Poland, 2019, pp. 1-4.

 ISBN: 978-1-61208-828-0